Thermodynamic Basis for Cluster Kinetics: Prediction of the Fragility of Marginal Metallic Glass-Forming Liquids

Lina Hu,*,† Xiufang Bian,† Xubo Qin,† Yuanzheng Yue,‡ Yan Zhao,† and Caidong Wang†

Key laboratory of Liquid Structure and Heredity of Materials, Ministry of Education, Shandong University (South Part), Jingshi Road 73, Jinan 250061, People's Republic of China, and Section of Chemistry, Aalborg University, Sohngaardsholmsvej 57, DK-9000 Aalborg, Denmark

Received: June 10, 2006; In Final Form: August 18, 2006

Due to the inaccessibility of the supercooled region of marginal metallic glasses (MMGs) within the experimental time window, we study the cluster kinetics above the liquidus temperature, T_l, to acquire information on the fragility of the MMG systems. The thermodynamic basis for the stability of locally ordered structure in the MMG liquids is discussed in terms of the two-order-parameter model. It is found that the Arrhenius activation energy of clusters, Δh, is proportional to the chemical mixing enthalpy of alloys, ΔH^{chem}. Fragility of the MMG forming liquids can be described by the ratio of the absolute ΔH^{chem} value to the glass transition temperature, T_g. The manner of vitrification during rapid solidification is an important factor for the discrepancy between the data presented in this paper and the prediction of the two-order-parameter model concerning the relation between Δh and the liquid fragility.

1. Introduction

Over the past decade the concept of liquid fragility has been attracting considerable attention from both materials scientists and physicists.[1−9] In particular, studies of liquid fragility have enhanced the understanding of the nature of the glass transition and the dynamics of glasses.[5] Extensive research on liquid fragility has been reported on different types of nonmetallic materials such as polymers, ionic glasses, and molecules.[6−17] These materials have demonstrated the connections between fragility and other physical properties of liquids,[10−17] and even between fragility and the properties of the corresponding solids at room temperature, e.g., elastic properties.[18] The direct connections of the kinetic fragility to the thermodynamic fragility and to the density of energy minima in a potential energy landscape (PEL) have been established.[12,13] Those correlations, however, have been explored on metallic systems to only a rather limited extent. Due to the importance of these systems in both fundamental research and potential applications,[19−21] liquid fragility is, recently, becoming one of the crucial subjects in the field of metallic materials.

As is well-known, metallic glass-forming liquids are often divided into two groups: bulk (such as Zr, Pd, Pt) and marginal (typically Al) systems.[22,23] The former generally have a large supercooled region of more than 150 K,[19] which enables one to investigate the dynamic properties of their supercooled liquids by such methods as dielectric relaxation and specific-heat measurements.[24,25] The bulk metallic glass (BMG) forming liquids are relatively strong,[26] and two important features in the PEL, i.e., the density of energy minima and the average height of barriers between minima, control the strength of their fragility.[27] In contrast, the latter systems, i.e., marginal metallic glass (MMG) forming liquids, exhibit peculiarities in many aspects. The BMGs usually possess the strongest glass-forming ability on the eutectic point or nearby.[28] Figure 1 shows that the composition ranges for the formation of an amorphous phase in Al-based systems, however, do not contain the eutectic point except in Al−Nd alloys.[29] Thermal scanning results of the MMGs also differ from those of the BMGs. For Al-based alloys the glass transition temperature, T_g, peak is hidden by the first crystallization peak.[30] Different phase transformations in the MMGs occur in the same temperature region if the heating rate is relatively low, whereas they occur in different temperature regions if the heating rate is relatively high. In other words, the separation of the temperature regions, where the transformations take place, becomes more and more pronounced with an increase in the heating rate. However, the confluence of the transformations in the BMGs could be observed at rather high heating rates.[31,32] The inaccessibility of the supercooled region of the MMGs prohibits the use of the detecting methods that are used for the BMGs.[33−35] Consequently, little work has been done on the dynamic properties of the MMGs near T_g and many questions concerning their liquid fragility remain unanswered.

In the present work, we search for the connections between the thermodynamic factors and the dynamic properties of Al-based liquid alloys. Thus we may find the dominant factor for the fragility of the MMG liquids. Earlier work[35] on amorphous solids well below T_g has qualitatively indicated the importance of cluster kinetics for understanding the nature of liquid fragility. Based on that work, we carry out semiquantitative investigations at the high-temperature end of supercooled regions, so that a close relationship between cluster kinetics in the liquid region and the chemical mixing enthalpy may be identified. In terms of such a relationship we also explore the possibility of predicting the fragility of MMGs.

2. Experimental Methods

The marginal alloys were prepared from a mixture of pure elements by arc melting under an argon atmosphere. Then the prealloyed ingots were remelted by high-frequency induction

* Corresponding author. Telephone: 086-531-88392748. Fax: 086-531-88395011. E-mail: hulina0850@mail.sdu.edu.cn.
† Shandong University.
‡ Aalborg University.

10.1021/jp063628q CCC: $33.50
Published on Web 10/06/2006

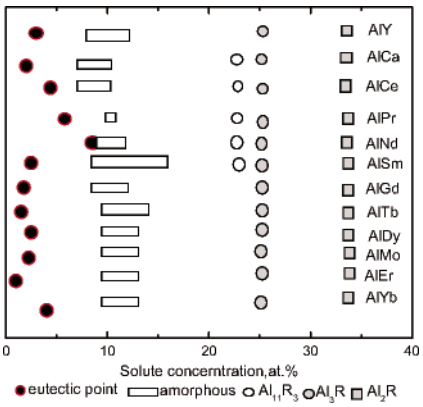

Figure 1. Composition ranges for the formation of an amorphous phase in Al-based systems.

and rapidly solidified into continuous ribbons by the single roller melt-spinning technique at a circumferential velocity of 2000 rev/min. The diameter of the copper roller was 35 cm. The thermal properties of the amorphous ribbons were investigated by a differential scanning calorimeter (DSC) (Netzsch DSC404) using pure indium (99.999 mass %) and zinc (99.999 mass %) standards and a sample mass of 20 ± 0.5 mg. All DSC measurements were conducted in a flowing (30 cm^3/min) nitrogen gas. The temperature error was ±2 K.

The liquid structures of MMGs were characterized by high-temperature X-ray wide-angle scattering, using a $\theta-\theta$ diffractometer and Mo Kα radiation, selected by a graphite monochromator. The liquid specimens of the AlCu alloys used in this work were put in an alumina crucible of size 8 mm × 25 mm × 30 mm in a high-purity helium atmosphere of 1.3×10^5 Pa, using Ta sheets as the heating elements. Every specimen was first overheated to 1573 K for 40 min. Then the specimen was cooled to the detection temperature and kept for 30 min for inherent equilibrium before the measurement was performed. The lowest detection temperature for each specimen was about 20−30 K higher than its T_l. The scanning voltage of the X-ray tube was 40 kV, the current was 30 mA, the exposure time was 30 s, and the measured 2θ angle was from 5° to 90°. The scattering intensity measured in arbitrary units can be converted into the coherent scattering intensity per atom in an electron unit, using the generalized Krogh−Moe−Norman method, with the atomic scattering factor including the anomalous dispersion factor.[36,37] Compton scattering is also corrected by using the values given by Cromer and Mann.[38] The detailed treatment of the scattering intensity data measured in arbitrary units and the error analysis of the $\theta-\theta$ liquid metal X-ray diffraction used in this experiment have been described elsewhere.[39,40] The amorphous character of the Al-based solid ribbons was confirmed by X-ray diffraction analysis. The experimental conditions were as follows: Cu Kα radiation, graphite monochromator, a voltage of 40 kV, a current of 100 mA, and a scattering angle range of $2\theta = 5°-80°$. The range of temperature error was ±2 K.

The liquid fragility can be determined using several thermal methods, one of which is the calculation of the activation energy for shear viscosity, ΔH^*, from calorimetric scanning rate dependence of T_g.[34] This method is based on the idea that glass transition occurs in the temperature region where a supercooled liquid deviates or returns to equilibrium and so, the same as viscosity, reflects the relationship between relaxation time and temperature. Accordingly, the value of ΔH^* for the MMGs was evaluated by eq 1:[35]

$$\ln \phi = -\Delta H^*/RT_{g,\phi} + \text{const} \quad (1)$$

where R is the gas constant; ϕ is the scanning heating rate; $T_{g,\phi}$ is the glass transition temperature at ϕ. A detailed experimental procedure to determine the value of ΔH^* by DSC has been described elsewhere.[35] The procedure requires that the experimental curve is recorded during the reheating process. The reheating rate ϕ ranges between 5 and 40 K/min. Before reheating the samples, the isothermal hold temperature for different glasses varied from 465 to 535 K, depending on their different T_x's. The well-known fragility index, m, was calculated by eq 2:[26,35]

$$m = \Delta H^*/RT_g \quad (2)$$

Although there are different definitions of T_g and different determination methods of T_g in the literature in eq 2,[1,6,12] the value of T_g by scanning calorimetry has been determined mostly at the reheating rate of 20 K/min for BMGs [26] or 10 K/min for nonmetallic materials.[1] It is believed that, at the scanning heating rate (10−20 K/min), the relaxation time at T_g approximates 100 s. To make convenient comparisons in m among alloys, $T_{g,20}$, the glass transition temperature at the heating rate of 20 K/min, was used here for the MMGs. In the following calculations, the T_g for the MMGs, which could not be probed directly, was replaced by the onset crystallization temperature, T_x, since both values are quite close to each other.

3. Results and Discussion

3.1. Stability of the Local Order Structure in Liquids and the Chemical Mixing Enthalpy of Marginal Alloys. Figure 2 shows the total structural factors $S(Q)$ of the liquid $Al_{100-x}Cu_x$ (x = 18, 25, 30, 35 in atoms) alloys at different temperatures ranging from 20 to 300 K above T_l. The pair distribution function $g(r)$ of the corresponding liquid alloys was obtained from the intensity of X-ray diffraction by Fourier transition, as shown in Figure 3. No distinct prepeaks are observed in the curves. The intensities of the main peak decrease with increasing temperature, indicating that the degree of order decreases as expected. Figure 4 shows the positions of the main peak of the liquid $Al_{100-x}Cu_x$ (x = 18, 25, 30, 35) alloys at different temperatures. The statistical error has been evaluated by the method developed by Egami.[41] The position of the main peak has a trend of shifting slightly toward smaller r-values with increasing Cu content, implying that the distance between atoms decreases slightly in real space. This phenomenon is expected from the effect of atomic size, since the Cu atomic radius (r_{Cu} = 1.28 Å) is smaller than that of Al (r_{Al} = 1.43 Å). The positions of the main peaks are independent of temperature for the AlCu alloys, which has also been observed for the AlFe liquids.[42]

A correlation between atomic structures of liquid alloys and the peculiarities of the phase equilibrium diagrams has been found in several laboratories.[43−46] Alloy melts consist of different types of crystal-like clusters distinguished by atomic packing and composition. The variation of melt composition within a certain region does not influence the existence of clusters of a certain type, but only changes their volumetric fraction. Accordingly, only the size of the locally ordered structure is a function of the melt temperature, rather than other structural parameters such as coordination number and the distance between the nearest atoms.[46]

The correlation radius of clusters in liquids, r_c, is often used to evaluate the size of the structurally ordered domain or the

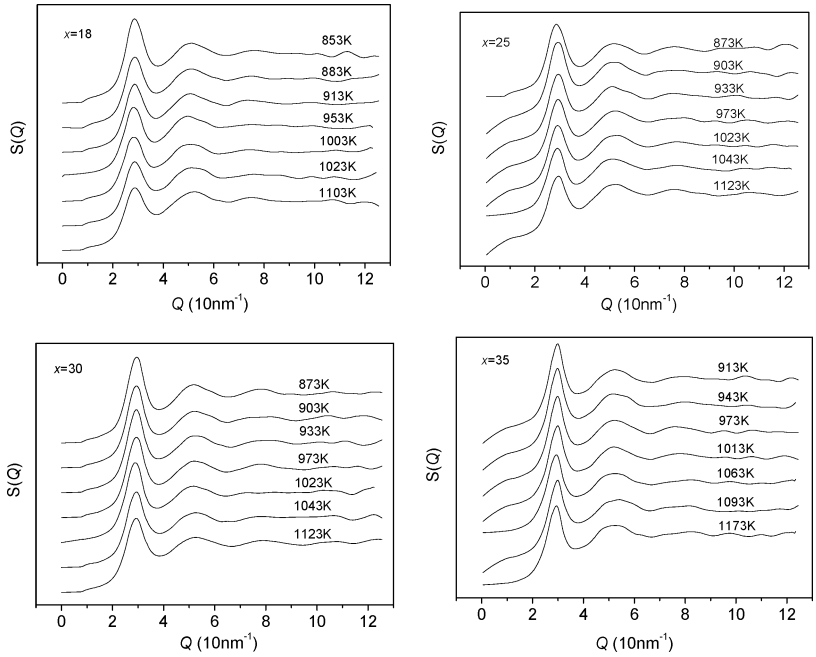

Figure 2. Total structure factors of four liquid $Al_{100-x}Cu_x$ (x = 18, 25, 30, 35) alloys at different temperatures.

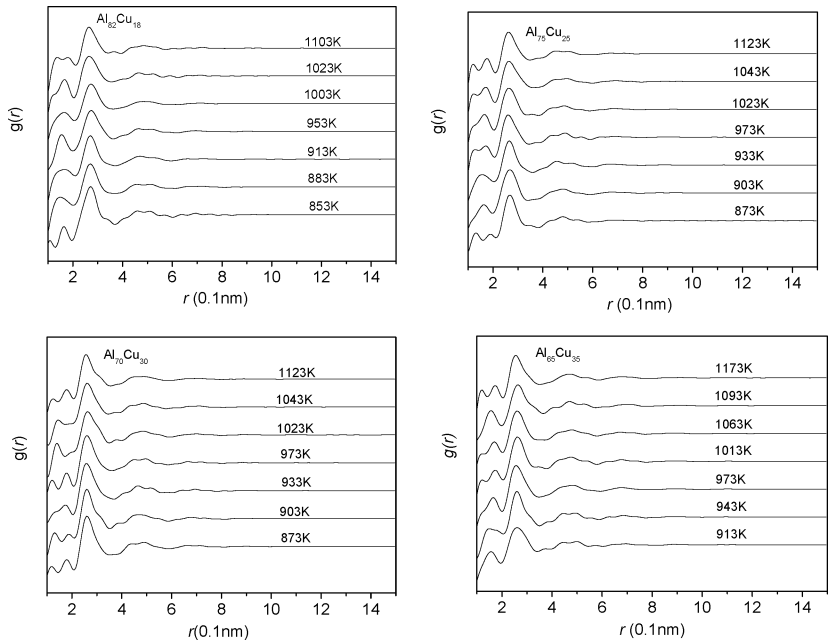

Figure 3. Pair distribution functions of $Al_{100-x}Cu_x$ (x = 18, 25, 30, 35) liquids at different temperatures.

degree of local order in liquids. In atomic distribution functions such as the pair distribution function $g(r)$ in Figure 3, the structurally ordered domain corresponds to the region where the density distribution of atomic number fluctuates. Theoretically, the correlation radius of clusters, r_c, is the minimum value of r where $g(r) = 1$, since $g(r) = 1$ means that the correlation disappears between the reference atom and other atoms.[39] Considering the experimental error and the error introduced by Fourier transition, however, the minimum value of r where $g(r) = 10.02$ is generally regarded as r_c.[47,48] Figure 5 illustrates the temperature dependences of r_c for the liquids of different $Al_{100-x}Cu_x$ (x = 18, 25, 30, 35) alloys. r_c shifts toward smaller values with increasing temperature. Different alloys exhibit different temperature dependences of r_c. At the same temperature an increase in the Cu content leads to an increase in r_c; i.e., the correlation radius of clusters increases even though large Al

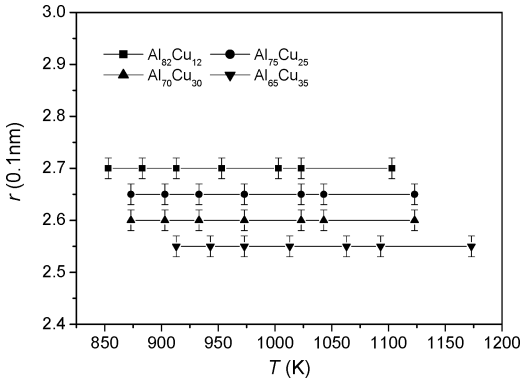

Figure 4. Position r of the main peak in the XRD spectra for the liquids of four $Al_{100-x}Cu_x$ (x = 18, 25, 30, 35) alloys at different temperatures.

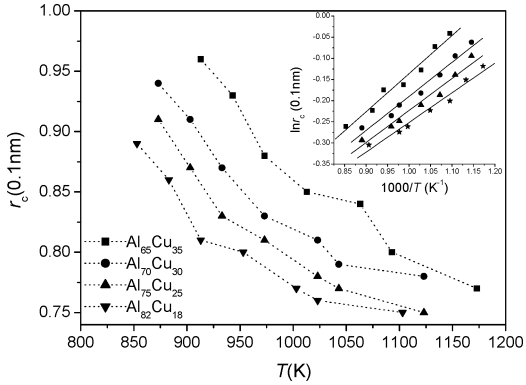

Figure 5. Correlation radius r_c in liquid $Al_{100-x}Cu_x$ ($x = 18, 25, 30, 35$) alloys as a function of temperature, T. The symbols stand for the experimental data, and the dotted lines are guides to the eye. The inset is the plot of ln r_c versus $1/T$. The solid lines represent the fitting of the experimental data to eq 3.

TABLE 1: Lattice Parameters of Some AlCu Alloys (Cu 18−35 atom %)

crystal	a (Å)	b (Å)	c (Å)
Al (cubic)	4.040		
Al_2Cu (tetragonal)	6.066		4.874
AlCu (monoclinic)	12.060	4.105	6.913

atoms are displaced by small Cu atoms. This means that a correlation between the atomic radius and the size of local order cannot be seen directly from Figure 4. According to the phase diagram, by increasing the Cu content from 18 to 31 atom %, it is expected that the fraction of Al atoms involved in the Al solid solution decreases, and hence, more clusters of similar Al_2Cu structure can form. When the Cu content reaches >31 atom %, clusters of similar AlCu compositions will be precipitated. The lattice parameters of the AlCu alloys with a Cu content between 18 and 35 atom % are listed in Table 1.[49,50] Obviously, the unit cell of the AlCu cluster is larger than that of Al_2Cu cluster, and the latter is larger than the unit cell of the Al cluster. These differences in size explain the increase in r_c with Cu additions.

We note that, as depicted by the dotted curves in Figure 5, the temperature dependence of r_c cannot be well described by a linear relationship. The increase in the average degree of local order with a decrease in temperature has been predicted by the two-order-parameter model of liquids.[51] The model relies on the physical picture wherein locally ordered structures with finite, but long, lifetimes are randomly distributed in a sea of normal-liquid structures. It assumes that there always exist two competing orderings in any liquids: density ordering leading to crystallization and bond ordering favoring a locally ordered structure. By introducing density order and bond order parameters, respectively, the locally ordered structures, which are energetically more favorable than normal-liquid structures, produce the effects of "fluctuating interactions" and "symmetry-breaking random field" against density ordering.[52] The model provides us with a universal view of glass transition from the strong to the fragile limit, even for multicomponent alloys.[51] According to the model, the temperature dependence of the correlation radius of clusters in liquids follows the Arrhenius law, as shown in Figure 6:

$$r_c = \Psi_0 \exp(\Delta h/RT) \tag{3}$$

where Ψ_0 and Δh are fitting parameters and T is temperature. Δh is regarded as the activation energy of clusters for the relaxation process, reflecting the stability of local order structure

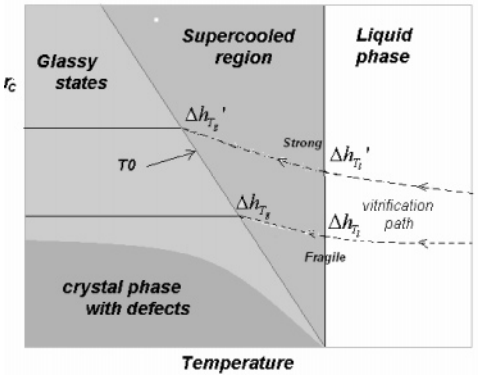

Figure 6. Changes of the strength of local order structure (expressed by r_c here) due to bond ordering during cooling. Δh_{T_l} and Δh_{T_g} are the activation energies reflecting cluster stabilities around T_l and T_g, respectively. According to the two-order-parameter model of liquids, $\Delta h_{T_l}'$ for strong liquids should be larger than Δh_{T_l} for fragile liquids, as the dashed lines shows.

TABLE 2: Fitting Parameters of Eq 3 [$r_c = \Psi_0 \exp(\Delta h/RT)$] for the AlCu Alloys near and above T_l[a]

alloys	Ψ_0	Δh (kJ/mol)	R
$Al_{82}Cu_{18}$	0.429	5.0	0.969
$Al_{75}Cu_{25}$	0.382	6.2	0.971
$Al_{70}Cu_{30}$	0.374	6.9	0.979
$Al_{65}Cu_{35}$	0.340	7.8	0.989

[a] R is the correlation factor for the linear relationship of ln $r_c \sim 1/T$.

in liquids. Note that eq 3 has the same form as another simple model of cluster kinetics by McCoy,[53] in which the Arrhenius activation energy, Δh, was displaced by the parameter of $h_m - h_c$. h_m is the energy needed for a particle separating from cluster, and h_c is the energy needed for cluster fusion. Although it remains unknown whether a correspondence exists between the two parameters (Δh and $h_m - h_c$) in the two different models, the validity of eq 3 has been confirmed by some experiments and numerical simulations.[54−56] The plot of ln r_c versus $1/T$ for the investigated AlCu alloys is shown in the inset of Figure 5. According to eq 3, a linear relationship is made for each alloy, and the fitting parameters derived from our experimental results are shown in Table 2. It is clearly seen that Ψ_0 decreases and contrarily Δh increases with raising the Cu content in the AlCu alloys. R is the correlation factor reflecting the fitting degree of the linear relationship of ln $r_c \sim 1/T$ to the experimental data, the maximum of which equals 1, representing the best quality of fitting. In Table 2, R ranges from 0.969 to 0.989. This indicates that the r_c-T relationship can be described by the Arrehnius law as shown in eq 3.

By performing molecular-dynamic simulations of simple metallic melts, Li et al. have realized that only the change in entropy with temperature controls the diffusion rate.[57] For complex multicomponent alloys, however, it seems that both the chemical mixing enthalpy, ΔH^{chem}, and the mismatch entropy, S_σ/k_B, which are temperature independent, play important roles in kinetics. The two correlated quantities determine not only the vitrification process via influencing the glass-forming ability (GFA) of alloys,[58] but also control the ease of structural relaxation of clusters for BMGs.[27] The question is what roles the two quantities play in cluster kinetics for marginal alloy liquids. Generally, the ΔH^{chem} value for binary and ternary

TABLE 3: Onset Temperature for the First Crystallization Peak ($T_{x,20}$), Chemical Mixing Enthalpy (ΔH^{chem}), Activation Enthalpy for Structural Relaxation (Δh), and Fragility Index (m) for $Al_{90-x}Ni_{10}Ce_x$ (x = 3, 5, 6, 8) Alloys[35]

alloy	$T_{x,20}$ (K)	ΔH^{chem} (kJ/mol)	Δh (kJ/mol)	m
$Al_{87}Ni_{10}Ce_3$	466	−11.96	3.5	57
$Al_{85}Ni_{10}Ce_5$	536	−14.50	10.6	95
$Al_{84}Ni_{10}Ce_6$	560	−15.72	15.6	141
$Al_{82}Ni_{10}Ce_8$	604	−18.08	20.5	209

amorphous alloys can be obtained by eq 4 on the basis of the extended regular solution model:[58]

$$\Delta H^{chem} = \sum_{\substack{i=1 \\ i \neq j}}^{n} \Omega_{ij} c_i c_j \quad (4)$$

where Ω_{ij} is the regular solution interaction parameter between the ith and jth elements; c_i is the composition of the i element; n is the total number of the elements. In the calculation of ΔH^{chem}, the mixing enthalpy ΔH_{ij}^{mix} resulting from Miedema's macroscopic model [59] for binary $i-j$ alloys was substituted for Ω_{ij} with the following relation: $\Omega_{ij} = 4\Delta H_{ij}^{mix}$. The prefactor 4 is due to the definition in eq 4 at the equiatomic composition in a binary $i-j$ system. The value of the mixing enthalpy ΔH_{ij}^{mix} was quoted from ref 59. According to eq 4, the ΔH^{chem} values of the AlCu alloys were calculated. In addition, the values of $|\Delta H^{chem}|$ for some AlNiCe alloys obtained by eq 4, as well as their values of Δh,[35] are listed in Table 3. Although the Δh value obtained for the AlCu alloys near and above T_l is different from that for the AlNiCe alloys, which was evaluated near T_g (denoted by Δh_{T_l} and Δh_{T_g}, respectively, in Figure 6), the continuous curve through the whole liquid region suggests that a large value of Δh_{T_l} corresponds to a large Δh_{T_g}. Besides, the well-known thermodynamic "Kauzmann plot" and the dynamic "Angell plot"[60] both suggest that no anomaly occurs at T_l and that the dynamics of the system continuously changes without any divergent behavior in liquid regions, with only a few exceptions such as water and silicon.[61]

When the absolute values of $|\Delta H^{chem}|$ are plotted against Δh for the AlCu and the AlNiCe alloys in Figure 7, a linear relationship is seen for both alloy systems. Although Δh shows different $|\Delta H^{chem}|$ dependences for the different alloy systems, a large Δh generally corresponds to large negative mixing enthalpy of the alloy. This means that the mixing enthalpy of alloys, which relates to the electronegativity and the difference in atomic size among component elements, is a key factor influencing the rate of structural relaxation of clusters. This finding may clarify why a large $|\Delta H^{chem}|$ corresponds to a small average height of energy barriers between the minima, $\Delta\mu$, for the BMGs.[27] The important role of the atomic diameter of the components in cluster kinetics accords with Mansoori's model, which describes the equilibrium thermodynamic properties of the mixture of hard spheres.[62] Besides, Figure 7 suggests that a large Δh will decease the stability of the clusters in marginal alloy melts. This agrees with what has been proposed by McCoy in his simple model,[53] in which a larger $h_c - h_m$ will lead to easier agglomeration of clusters during cooling. Thus, a correspondence between the two parameters of Δh and $h_c - h_m$ has been found for the MMGs, though the assumptions of the two-order-parameter model are quite different from those of the simple one.

3.2. Liquid Fragility of MMGs and Their Potential Energy Landscape. Considering the strong Δh dependence of $|\Delta H^{chem}|$ in Figure 7, as well as the relationship between cluster kinetics and liquid fragility,[53,60] we plot the fragility parameter, m, against the values of $|\Delta H^{chem}|/T_{g,20}$ for some AlNiCe alloys in Figure 8. Here $T_{x,20}$ is used instead of $T_{g,20}$ due to the usual difficulty in detecting T_g for Al-based alloys and because the value of T_x is close to that of T_g.[33] The values of m and $T_{x,20}$ are listed in Table 3.[35]

The relationship $m \sim |\Delta H^{chem}|/T_{x,20}$ is fitted by a linear equation. As seen from Figure 8, the AlNiCe alloy system exhibits a linear relationship between the two quantities with the slope of $k = 36.3$. The correlation factor, R, is 0.997. To discover whether the linear relationship is general for the MMGs, we need to obtain more fragility parameters of marginal alloys. Here we select the AlCoCe alloy system.

Figure 9 shows the DSC curves at a heating rate of 20 K/min of the $Al_{90-x}Co_{5+x}Ce_5$ (x = 0, 3, 5) samples which were spun at a circumferential velocity of about 2000 rev/min. X-ray

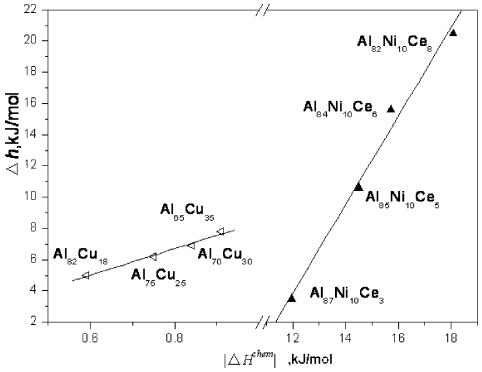

Figure 7. Activation energy for structural relaxation of clusters, Δh, versus absolute value of chemical mixing enthalpy, $|\Delta H^{chem}|$, for AlNiCe and AlCu alloys.

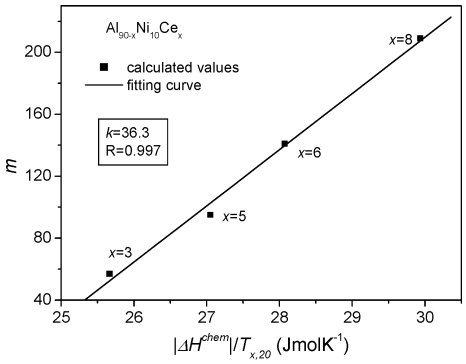

Figure 8. Fragility index m versus $|\Delta H^{chem}|/T_{g,20}$ for the $Al_{90-x}Ni_{10}Ce_x$ (x = 3, 5, 6, 8) metallic system. $T_{x,20}$ is used instead of $T_{g,20}$ here. k is the slope of the fitting linear relationship.

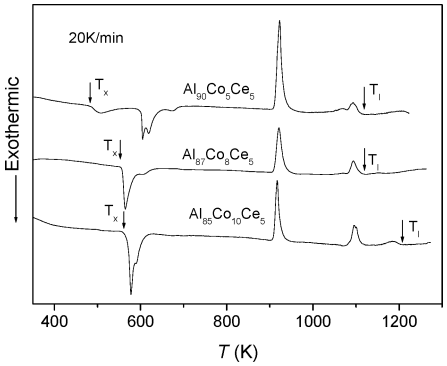

Figure 9. Differential scanning calorimetry (DSC) output as a function of temperature for $Al_{90-x}Co_{5+x}Ce_5$ samples (x = 0, 3, 5) at scanning heating rate of 20 K/min.

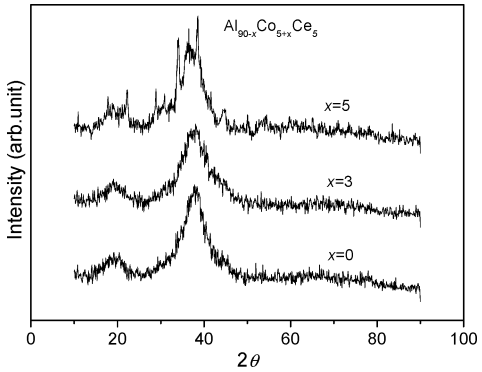

Figure 10. X-ray diffraction (XRD) patterns of $Al_{90-x}Co_{5+x}Ce_5$ (x = 0, 3, 5) systems.

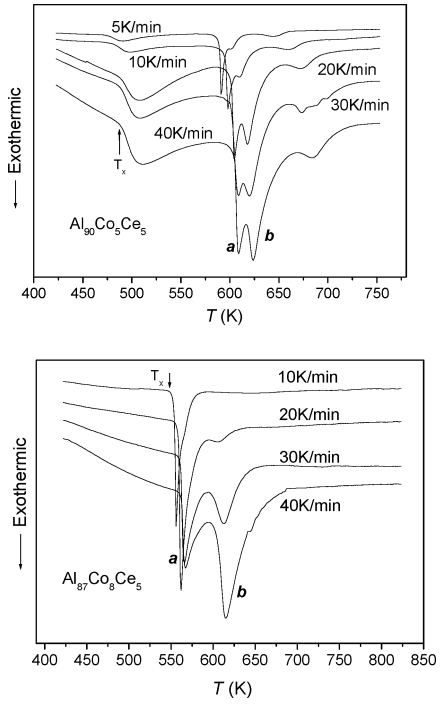

Figure 11. DSC output as a function of temperature for $Al_{90}Co_5Ce_5$ and $Al_{87}Co_8Ce_5$ glasses at different heating rates.

diffraction intensities of the samples are shown in Figure 10. No crystal diffraction peaks are detected in the $Al_{90-x}Co_{5+x}Ce_5$ (x = 0, 3) curves. The broad diffraction peaks indicate full vitrification of the two samples. For the $Al_{85}Co_{10}Ce_5$ sample, a few sharp diffraction peaks appear, indicating the mixture of dispersed crystal matrix and amorphous background. A prepeak is observed around $2\theta = 20°$ for all three samples. For $Al_{85}Co_{10}Ce_5$, however, the sharp diffraction peaks are superimposed on the prepeak. This implies that the medium-range order structure in $Al_{85}Co_{10}Ce_5$ leading to the prepeak is unstable compared to that in $Al_{90}Co_5Ce_5$ and $Al_{87}Co_8Ce_5$.

DSC curves of the amorphous $Al_{90}Co_5Ce_5$ and $Al_{87}Co_8Ce_5$ alloys at different heating rates are shown in Figure 11 as examples. The values of T_x for each sample at different heating rates, ϕ, as well as the calculated values of ΔH^* and m, have been listed in Table 4. It has been found that eq 1 presents a good description of the $\log \phi \sim 1/T_{x,\phi}$ relation for all the AlCoCe alloys. The values of m and ΔH^* both increase approximately 3 times by increasing the Co content from 5 to 10 atom %. The values of ΔH^{chem} calculated for the AlCoCe system are given in Table 4.

According to Table 4, the fragility increases with an increase in the value of $|\Delta H^{chem}|$. The plot of the fragility index m versus

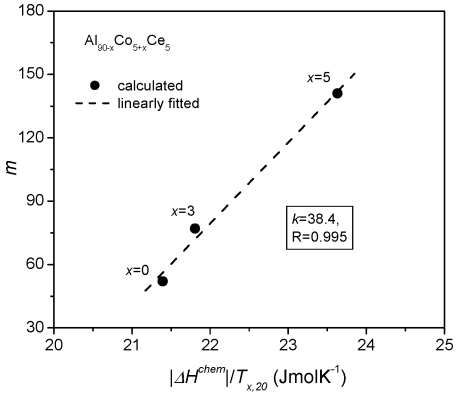

Figure 12. Fragility index m versus $|\Delta H^{chem}|/T_{x,20}$ for $Al_{90-x}Co_{5+x}Ce_5$ (x = 0, 3, 5) metallic system.

TABLE 4: Values ($T_{x,\phi}$, ΔH^*, and m) Obtained by Thermal Scanning Experiments of $Al_{90-x}Co_{5+x}Ce_5$ (x = 0, 3, 5) Alloys

	$T_{x,\phi}$ (K)					ΔH^*		ΔH^{chem}
sample	$T_{x,5}$	$T_{x,10}$	$T_{x,20}$	$T_{x,30}$	$T_{x,40}$	(kJ/mol)	m	(kJ/mol)
$Al_{90}Co_5Ce_5$	473	481	488	490	492	207	52	−10.44
$Al_{87}Co_8Ce_5$		553	559	561	563	358	77	−12.19
$Al_{85}Co_{10}Ce_5$	557	559	562	564	565	659	141	−13.28

$|\Delta H^{chem}|/T_{x,20}$ is shown in Figure 12. The correlation between the two quantities is described by a linear function with a correlation factor of 0.995. Thus, the AlCoCe alloy system exhibits the same behavior as the AlNiCe alloys. This again verifies the reasonableness of the linear relationship between the fragility and the T_x scaled mixing enthalpy. In fact, T_x in Figure 12 reflects the link between the glass transition temperature and liquid fragility, since for the AlCoCe alloys T_g is undistinguishable from T_x, but rather close to T_x, as shown in Figure 11. In Figures 8 and 12, the slope of the m versus $|\Delta H^{chem}|/T_{x,20}$ curve, k, is equal to 36.3 for AlNiCe and to 38.4 for the AlCoCe system. However, in this work it is not possible to conclude whether the difference in the value of k is due to different systems or experimental errors.

Consequently, the liquid fragility denoted by m can be formulated as

$$m \propto k\Delta H^{chem}/T_g \tag{5}$$

As stated above, $T_{x,20}$ is approximately regarded as T_g. Equation 5 implies that the T_g normalized chemical mixing enthalpy governs the liquid fragility for MMGs, since k is a constant parameter. To analyze the physical origin of this implication, we should refer to the following existing knowledge. T_g reflects the level of the PEL, at which the system gets trapped during cooling. A higher fragility index, m, corresponds to a larger jump in heat capacity from glass to liquid state, ΔC_p, for most nonmetallic systems (such as polymers, inorganic glasses, ionic liquids, and small molecules) and even recently BMGs.[27,63−65] The density of energy minima in the PEL was, if not unique, at least one of the dominant factors that control the liquid fragility.[66,67] The group of MMGs, however, exhibits a very different behavior. The fragility of marginal alloy liquids is determined solely by the average height of energy barriers between minima according to the relation $|\Delta H^{chem}| \propto 1/\Delta\mu$. The density of energy minima is not a significant factor in influencing the fragility of the MMG systems. On the basis of the results shown in Figure 7, it can be stated that m and ΔH^{chem} are linearly linked as described by eq 5. This relation is derived from the fact that the fragility index, m, is proportional to the activation

energy of structural relaxation of clusters in liquids, Δh, and the latter is linearly related to the mixing enthalpy, ΔH^{chem}.

Furthermore, the following phenomenon is also striking. According to the two-order-parameter model, a system with a strong tendency to form locally ordered structures in liquids, which causes an extra energy barrier for crystal nucleation, should have a large value of Δh and make vitrification easy. For example, the icosahedral clusters of 13 particles that exist in alloy liquids have significantly lower energy than "crystallographic" arrangements.[68] As a result, Δh is larger, hence, the stability of the clusters is higher, and the liquid becomes stronger (see the dashed lines in Figure 6). Although some authors support this view,[69−71] the results obtained in the present work show a different case; i.e., the marginal alloys with large Δh involve unstable clusters and large fragility. These results agree with the prediction of the simple model by McCoy,[53] implying that the locally ordered structures with bond ordering do not always hamper the occurrence of crystallization. For the MMGs these structures tend to destabilize the supercooled liquids, as experimentally verified in Figure 5. Increasing the Cu content leads to an increase in the degree of local structural order of the liquids. At the same time, the correlation radius changes more rapidly with temperature by increasing the Cu content. This means that the stability of clusters decreases, accompanied by an increase in the degree of the local order.

According to nonclassical nucleation theories (such as the diffuse interface theory by Granasy[72] and the semiempirical density functional approximation by Bagdassarian[73]), the locally ordered structure preexisting in the supercooled liquid tends to act as a nucleus during solidification, and then make the amorphous structure unstable. It should be noted that the key point of nonclassical nucleation theories is that the vitrification process during cooling is diffusion controlled. In the diffusion-controlled case, a larger Δh means a larger quantity of clusters acting as nuclei to relax themselves, resulting in the instability of supercooled liquids. It has been found that the vitrification of the AlNiCe, AlNiZr, and AlNiCuCe alloys is diffusion-controlled.[74] In contrast, in the nucleation-controlled vitrification, it is expected that the larger the Δh value is, the more energy is required to transform the locally favored structures into nuclei, making the supercooled liquid more stable. This case agrees with the prediction by the two-order-parameter model. The vitrification process (diffusion-controlled or nucleation-controlled) is dependent on the degree of dissimilarity between the structures of the first precipitates and the locally ordered structure of the liquid.[75] If the icosahedral characteristic bond pairs (such as 1311, 1321, 1551, and 1541) are difficult to transfer into crystal characteristic bond pairs (such as 1421, 1661, 1441, and 1422), the supercooled liquids of the alloys are strong.[76,77]

4. Conclusions

The fragility index for the MMGs can be predicted in terms of the ratio of mixing enthalpy of alloys to the glass transition temperature. Different from the BMGs and nonmetallic materials, MMG materials with poor glass-forming ability exhibit a unique dependence of liquid fragility on the average height of the energy barriers between minima. This unusual phenomenon is attributed to the linear relationship between the mixing enthalpy of alloys and the activation energy for the relaxation of clusters, which reflects the stability of locally ordered structures in liquids. Although the mixing enthalpy is a static value and the activation energy is a dynamic value, their correlation suggests a common physical origin. This finding is helpful for clarifying what leads to different dynamic behaviors of liquids. In addition, for the MMGs, the randomly distributed clusters with local order in liquids result in the instability of supercooled liquids. This phenomenon is unexpected from the two-order-parameter model. The disagreement between the results obtained in the present work and the model closely relates to the difference in vitrification mechanism for different metallic glass-forming liquids.

Acknowledgment. This work was supported by the National Natural Science Foundation of China (Grant. 50231040), the Doctoral Program Foundation of Institutions of Higher Education of China (Grant 20050422024), and the Natural Science Foundation of Shandong Province (Project No. Z2004F02).

References and Notes

(1) Angell, C. A. *Science* **1995**, *267*, 1924.
(2) Sudha, S.; Shankar, P. *Phys. Lett. A* **2001**, *286*, 76.
(3) Moreno, A. J.; Buldyrev, S. V.; Nave, E. La.; Saika-Voivod, I.; Sciortino, F.; Tartaglia, P.; Zaccarelli, E. *Phys. Rev. Lett.* **2005**, *95*, 15802.
(4) Sokolov, A. P.; Rossler, E.; Kisliuk, A.; et al. *Phys. Rev. Lett.* **1993**, *71*, 2062.
(5) Angell, C. A. *J. Phys. Chem. B* **1999**, *103*, 3977.
(6) Roland, C. M.; Santangelo, P. G.; Ngai, K. L. *J. Chem. Phys.* **1999**, *111*, 5593.
(7) Green, J. L.; Ito, K.; Xu, K.; Angell, C. A. *J. Phys. Chem. B* **1999**, *103* (20), 3991.
(8) Moriya, K.; Matsuo, T.; Suga, H.; et al. *Chem. Lett. (Jpn.)* **1977**, *58*, 1427.
(9) Ito, K.; Moynihan, C. T.; Angell, C. A. *Nature* **1999**, *398*, 492.
(10) Huang, D. H.; Gregory, B. M. *J. Chem. Phys.* **2001**, *114*, 5621.
(11) Ngai, K.; Yamamuro, O. *J. Chem. Phys.* **1999**, *111*, 10403.
(12) Martinez, L. M.; Angell, C. A. *Nature* **2001**, *410*, 663.
(13) Sciortino, F.; Kob, W.; Tartaglia, P. *Phys. Rev. Lett.* **1999**, *83*, 3214.
(14) Michael, S. *Phys. Rev. B* **1998**, *57*, 11319.
(15) Scopigno, T.; Giancarlo, R.; Francesco, S.; Giulio, M. *Science* **2003**, *302*, 849.
(16) Rossler, E.; Sokolov, A. P. *Chem. Geol.* **1996**, *128*, 143.
(17) Yannopoulos, S. N.; Papatheodorou, G. N. *Phys. Rev. B* **2000**, *62*, 3728.
(18) Novikov, V. N.; Sokolov, A. P. *Nature* **2004**, *431*, 903.
(19) Inoue, A. *Acta Mater.* **2000**, *48*, 279.
(20) Rösner, P.; Samwer, K.; Lunkenheimer, P. *Europhys. Lett.* **2004**, *68*, 226.
(21) Zhang, B.; Pan, M. X.; Zhao, D. Q.; Wang, W. H. *Appl. Phys. Lett.* **2004**, *85*, 61.
(22) Wilde, G.; Boucharat, N.; Hebert, R. J.; Rösner, H.; Tong, W. S.; Perepezko, J. H. *Adv. Eng. Mater.* **2003**, *5*, 125.
(23) John, H. P.; Rainer, J. H. *JOM* **2002**, *54* (3), 34.
(24) Wen, P.; Zhao, D. Q.; Pan, M. X.; Wang, W. H. *Appl. Phys. Lett.* **2004**, *84*, 2790.
(25) Johnson, W. L. *MRS Bull.* **1999**, *24*, 42.
(26) Perera, D. N. *J. Phys.: Condens. Matter* **1999**, *11*, 3807.
(27) Hu, L. N.; Bian, X. F.; Wang, W. M.; Liu, G. R.; Jia, Y. B. *J. Phys. Chem. B* **2005**, *109*, 13737.
(28) Davis, H. A. In *Amorphous Metallic alloys*; Luborsky, F. E., Ed.; Butterworth: London, 1983.
(29) Inoue, A.; Zhang, T.; Kita, K.; Masumoto, T. *Mater. Trans., JIM* **1989**, *30*, 870.
(30) Sa-Lisboa, R. D.; Kiminami, C. S. *J. Non-Cryst. Solids* **2002**, *304*, 36. Zhang, B.; Bian, X. F.; Si, P. C.; Zhou, J. K.; Lin, T.; Jia, Y.B. *Phys. Lett. A* **2004**, *327*, 38.
(31) Louzguine, D. V.; Inoue, A. *J. Non-Cryst. Solids* **2002**, *311*, 281. Louzguine, D. V.; Inoue, A. *Mater. Res. Bull.* **1999**, *34*, 1991.
(32) Louzguine, D. V.; Inoue, A.; Saito, M.; Waseda, Y. *Scr. Mater.* **2000**, *42*, 289. Louzguine, D. V.; Inoue, A. *Scr. Mater.* **2000**, *43*, 371.
(33) Inoue, A. *Prog. Mater. Sci.* **1998**, *43*, 365. Ye, F.; Lu, K. *J. Non-Cryst. Solids* **2000**, *262*, 228.
(34) Moynihan, C. T. *Rev. Mineral.* **1995**, *32*, 1. Crowley, K. J.; Zografi, G. *Thermochim. Acta* **2001**, *380*, 79.
(35) Hu, L. N.; Bian, X. F.; Wang, W. M,.; Zhang, J. Y.; Jia, Y. B. *Acta Mater.* **2004**, *52*, 4773.
(36) Wasada, Y. *The Structure of Non-Crystalline Materials*; McGraw-Hill: New York, 1980; p 10.
(37) *37.International Tables for X-ray Crystallography*; Kynoch: Birmingham, 1974; p 74.
(38) Cromer, D. T.; Mann, J. B. *J. Chem. Phys.* **1967**, *47*, 1892.

(39) Buhalenko, V. V.; Il'inskii, A.; Romanova, A. V. *Metallofizika* **1991**, *13*, 92.
(40) Giessen, B. C.; Wagner, C. N. J. *Liquid Metals*; Marcel Dekker: New York, 1972.
(41) Egami, T. *Mater. Sci. Eng., A* **1994**, *179&180*, 17.
(42) Zhang, L.; Wu, Y. S.; Bian, X. F.; Li, H.; Wang, W. M.; Wu, S. *J. Non-Cryst. Solids* **2000**, *262*, 169.
(43) Qin, J. Y.; Bian, X. F.; Sliusarenko, S. I.; Wang, W. M. *J. Phys.: Condens. Matter* **1998**, *10*, 1211.
(44) Gebhardt, B.; Halm, T.; Hoyer, W. *J. Non-Cryst. Solids* **1995**, *192&193*, 306. Il'inskii, A.; Kaban, I.; Slyusarenko, S.; Hoyer, W. *Metallofizika* **1993**, *15*, 42.
(45) Il'inskii, A.; Slyusarenko, S.; Slukhovskii, O.; Kaban, I.; Hoyer, W. *Mater. Sci. Eng., A* **2002**, *325*, 98.
(46) Il'inskii, A.; Slyusarenko, S.; Slukhovskii, O.; Kaban, I.; Hoyer, W. *J. Non-Cryst. Solids* **2002**, *306*, 90.
(47) Huang, S. T. *The structure of non-crystalline materials and structural analysis*; Science Press: Beijing, 1987; p 263.
(48) Tian, X. L.; Chen, X. C.; Il'inskii, A. *Sci. China, Ser. A* **2000**, *43*, 1301.
(49) Bradley, J. *J. Inst. Met.* **1933**, *51*, 131.
(50) El-Boragy, M.; Szepan, R. *J. Less-Common Met.* **1972**, *29*, 133.
(51) Tanaka, H. *J. Phys.: Condens. Matter* **1998**, *10*, L207. Tanaka, H. *J. Phys.: Condens. Matter*. **2003**, *15*, L491.
(52) Tanaka, H. *J. Chem. Phys.* **1999**, *111*, 3163.
(53) McCoy, B. J. *J. Phys. Chem. Solids* **2002**, *63*, 1967.
(54) Tanaka, H. *Phys. Rev. Lett.* **1998**, *80*, 5750. Tanaka, H. *J. Chem. Phys.* **2000**, *112*, 799.
(55) Tanaka, H. *Phys. Rev. B* **2002**, *66*, 064202.
(56) Tomida, T.; Egami, T. *Phys. Rev. B* **1995**, *52*, 3290.
(57) Li, G. X.; Liu, C. S.; Zhu, Z. G. *Phys. Rev. B* **2005**, *71*, 094209.
(58) Takeuchi, A.; Inoue, A. *Mater. Trans., JIM* **2000**, *41*, 1372.
(59) Boer, F. R.; Perrifor, D. G. *Cohesion in Metals*; Elsevier: Amsterdam, The Netherlands, 1988.
(60) Angell, C. A. *J. Non-Cryst. Solids* **1985**, *73* (1−3), 1. Angell, C. A. *J. Res. Natl. Inst. Stand. Technol.* **1997**, *102*, 171.
(61) Angell, C. A. *Chem. Rev.* **2002**, *102*, 2627.
(62) Mansoori, G. A.; Carnahan, N. F.; Starlino, K. E.; Leland, J. T. W. *J. Chem. Phys.* **1971**, *54*, 1523.
(63) Angell, C. A. *J. Non-Cryst. Solids* **1988**, *102* (1−3), 205. Debenedetti, P. G.; Stillinger, F. H. *Nature* **2001**, *410*, 259.
(64) Böhmer, R.; Ngai, K. L.; Angell, C. A.; Plazek, D. J. *J. Chem. Phys.* **1993**, *99*, 4201.
(65) Angell, C. A. *J. Non-Cryst. Solids* **2002**, *307−310*, 393.
(66) Speedy, R. J. *J. Phys. Chem. B* **1999**, *103*, 4060.
(67) Sastry, S. *Nature (London)* **2001**, *409*, 164.
(68) Frank, F. C. *Proc. R. Soc. London, Ser. A* **1952**, *215*, 43.
(69) Kelton, K. F.; Lee, G. W.; Gangopadhyay, A. K.; Hyers, R. W.; et al. *Phys. Rev. Lett.* **2003**, *90*, 195504.
(70) Yan, Z. J.; Li, J. F.; He, S. R.; Zhou, Y. H. *Mater. Lett.* **2003**, *57*, 1840.
(71) Park, C.; Saito, M.; Wasedam, Y. *Mater. Trans., JIM* **1999**, *40*, 491.
(72) Granasy, L. *Mater. Sci. Forum* **1996**, *215−216*, 451.
(73) Bagdassarian, C. K.; Oxtoby, D. V. *J. Chem. Phys.* **1994**, *100*, 2139.
(74) Tsai, A. P.; Kamiyama, T.; Kawamura, Y.; Inoue, A.; Masumoto, T. *Acta Mater.* **1997**, *45*, 1477.
(75) Xing, L. Q.; Hufnagel, T. C.; Eckert, J.; Loser, W.; Schulta, L. *Appl. Phys. Lett.* **2000**, *77*, 1970.
(76) Liu, C. S.; Zhu, Z. G.; Xia, J. C.; Sun, D. Y. *J. Phys.: Condens. Matter* **2001**, *13*, 1873.
(77) Li, H.; Pederiva, F. *Phys. Rev. B* **2003**, *68*, 054210.